**Supporting Information**

# A biomineralized bi-functional hybrid nanoflower to effectively combat bacteria *via* a glucose-powered cascade catalytic reaction

*Qiaorong Tang, Lu Shi, Bing Yang, Wei Liu, Baoxin Li, and Yan Jin**

Key Laboratory of Analytical Chemistry for Life Science of Shaanxi Province, Key Laboratory of Applied Surface and Colloid Chemistry, Ministry of Education, School of Chemistry and Chemical Engineering, Shaanxi Normal University, Xi'an 710119, China.

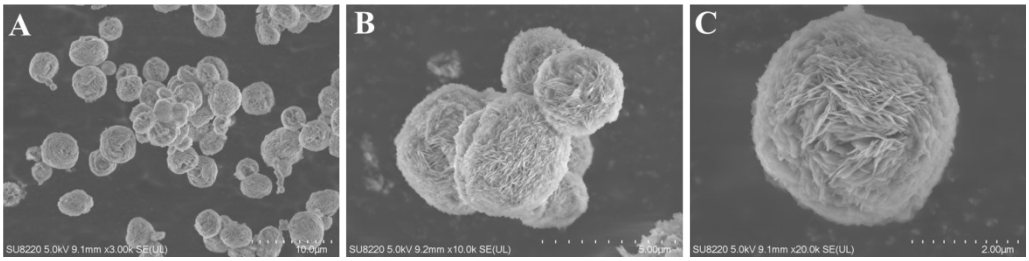


**Figure S1.** SEM images of Cu-GMPNF (A-C).

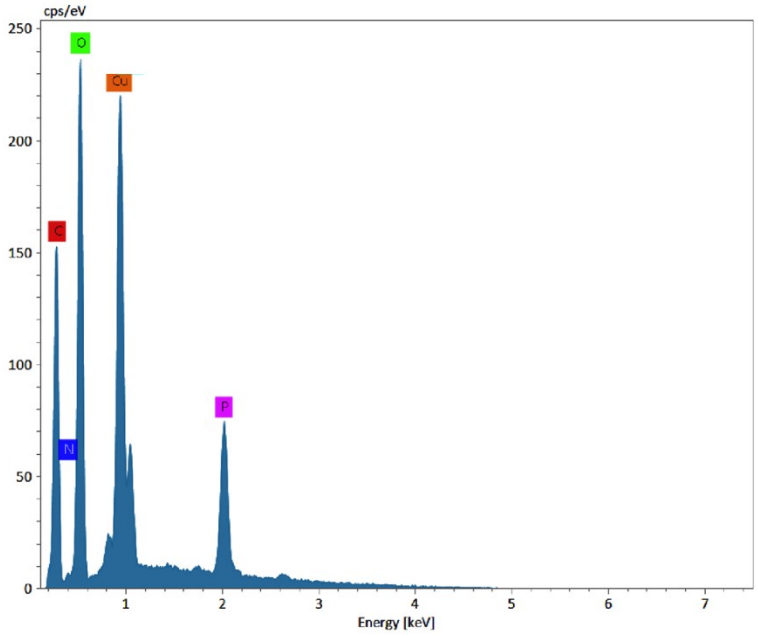


**Figure S2.** EDS of Cu-GMP/GODNF

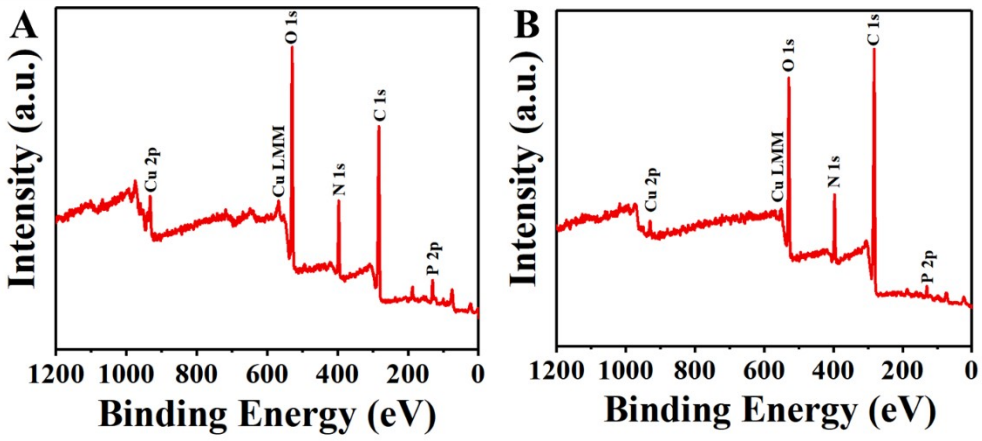


**Figure S3.** XPS spectra of Cu-GMPNF (A) and Cu-GMP/GODNF (B)

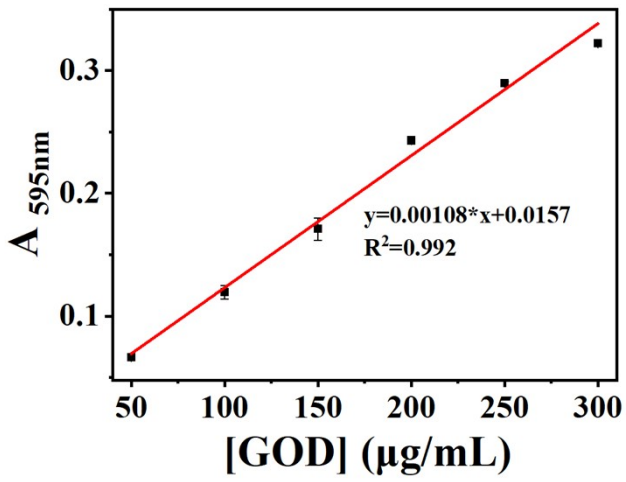


**Figure S4.** Calibration curves for different concentrations of GOD solutions (50 ~ 300 μg · $mL^{-1}$) according to Modified Bradford Protein Assay Kit.

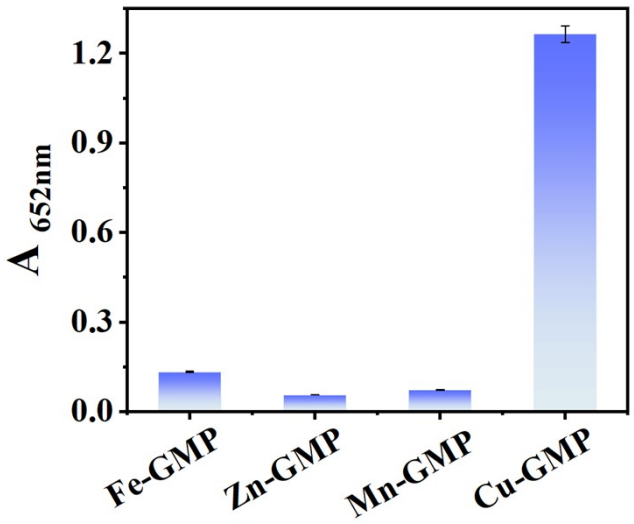


**Figure S5.** The POD-like activity of different metal/GMP (0.1 mg/mL) by measuring the absorbance of oxTMB at 652 nm under 2.0 mM $H_2O_2$ (NaAc-HAc buffer, pH 5.0).

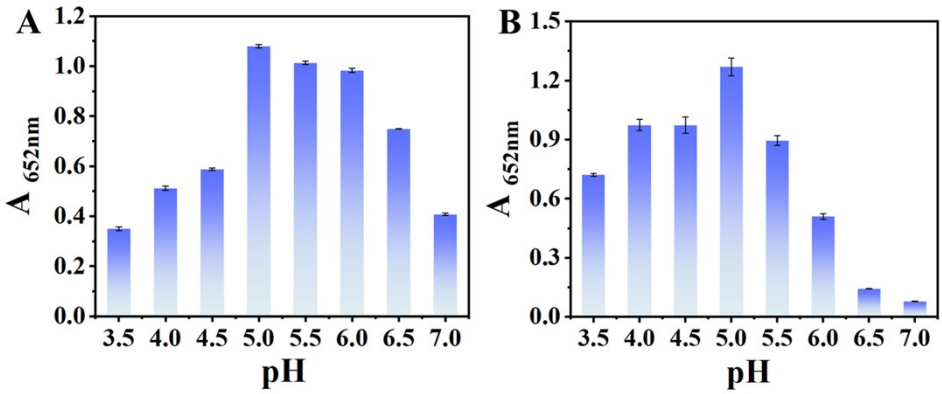


**Figure S6**. pH-dependence POD-like activity of Cu-GMPNF and cascade catalytic activity of Cu-GMP/GODNF.

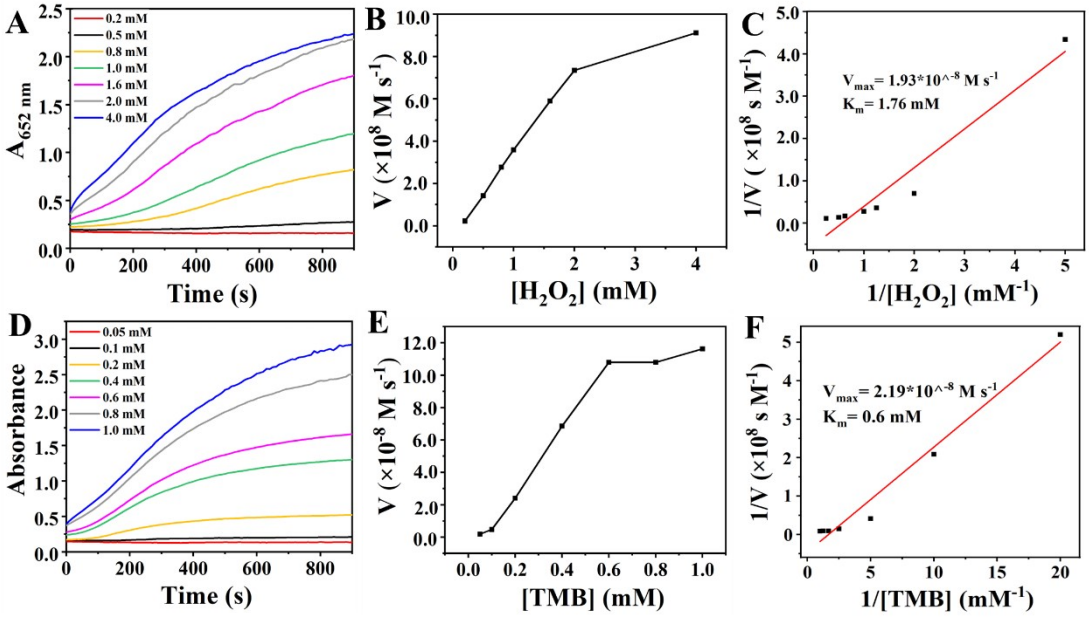


**Figure S7**. Typical Michaelis-Menten curves and kinetic parameters of Cu-GMPNF. Absorbance at 652 nm vs time of reaction solutions catalyzed by the Cu-GMPNF under different concentrations of $H_2O_2$ (A) or TMB (D). The velocity (v) of the reaction changes in the presence of different concentrations of $H_2O_2$ (B) or TMB (E). The double-reciprocal plot in the presence of different concentrations of $H_2O_2$ (C) or TMB (F). All experiments were conducted in 1.0 mg/mL of Cu-GMPNF. When the $H_2O_2$ concentration was varied, the TMB concentration was fixed at 1.0 mM. When the TMB concentration was varied, the $H_2O_2$ concentration was fixed at 5.0 mM.

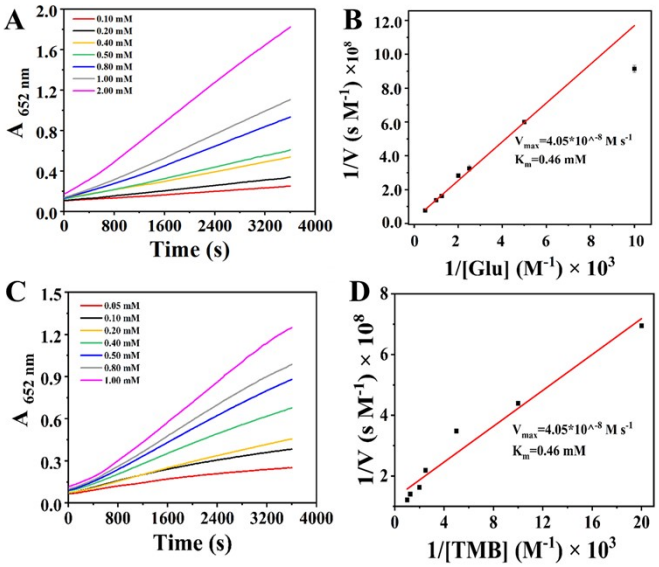


**Figure S8**. Steady-state kinetic data of the Cu-GMP/GODNF. Absorbance at 652 nm vs time of reaction solutions catalyzed by the Cu-GMP/GODNF under different concentrations of glucose (A) or TMB (D). Velocity (v) of the reaction changes in the presence of different concentrations of glucose (B) or TMB (E). Double-reciprocal plot in the presence of different concentrations of glucose (C) or TMB (F).

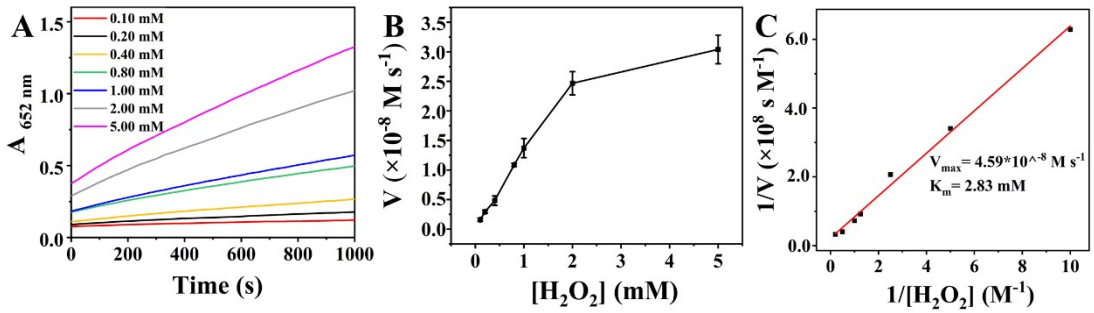


**Figure S9**. Typical Michaelis-Menten curves and POD-like kinetic parameters of Cu-GMP/GODNF. Absorbance at 652 nm vs time of reaction solutions catalyzed by the Cu-GMP/GODNF under different concentrations of $H_2O_2$ (A). The velocity (v) of the reaction changes in the presence of different concentrations of $H_2O_2$ (B). The double-reciprocal plot in the presence of different concentrations of $H_2O_2$ (C). All experiments were conducted in 1.0 mg/mL of Cu-GMP/GODNF. When the $H_2O_2$ concentration was varied, the TMB concentration was fixed at 1.0 mM.

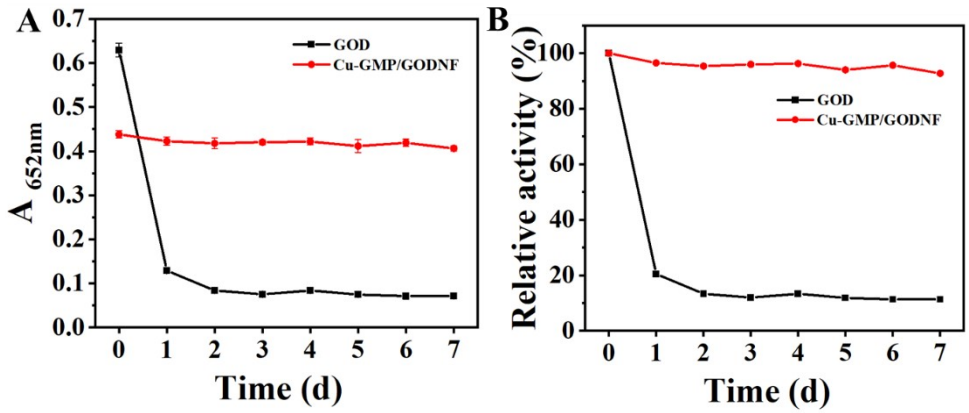


**Figure S10**. Absorbance of free GOD + Cu-GMPNF or Cu-GMP/GODNF catalyzed glucose/TMB at 652 nm (A), catalytic activity of free GOD and Cu-GMP/GODNF (B) under different storage times.

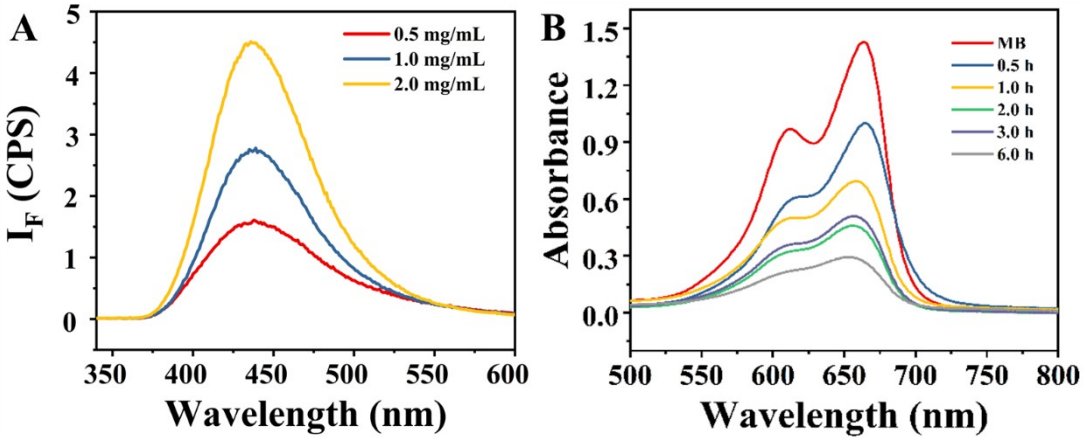


**Figure S11**. TA fluorescent signal generated with increasing Cu-GMP/GODNF concentration at 435 nm (A). The degradation of MB at different time points (B).

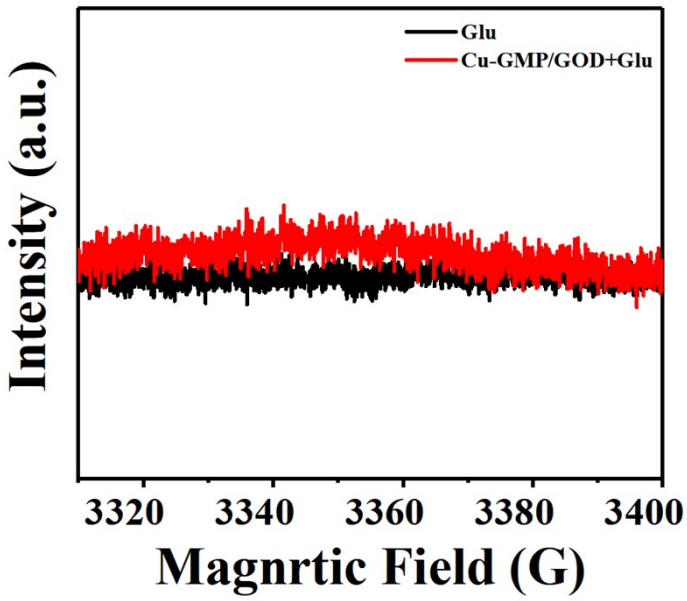


**Figure S12**. ESR spectra of different reaction systems with and $^1O_2$.

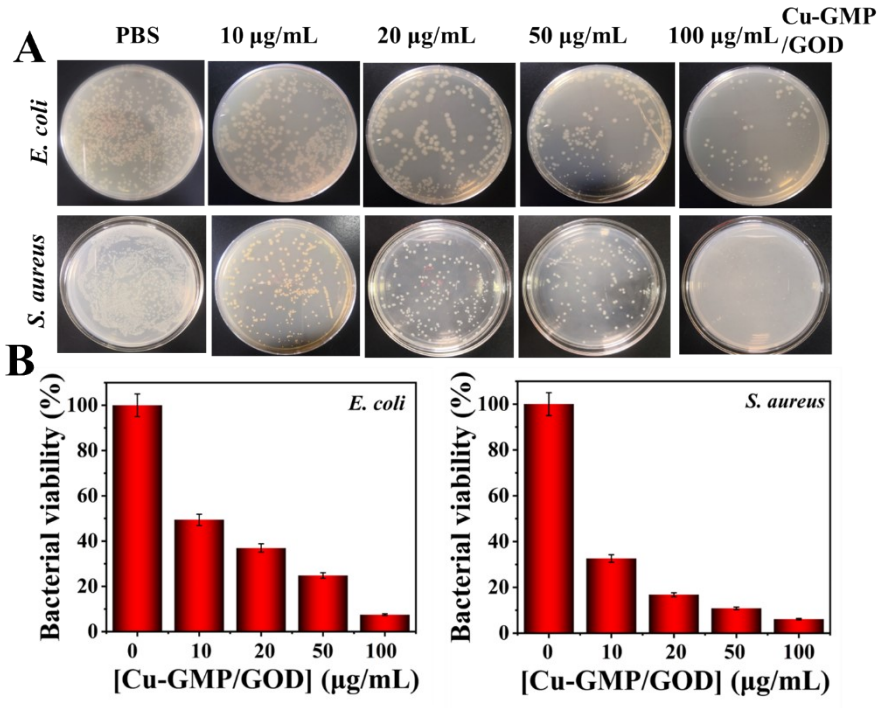


**Figure S13**. Agar plate results (A) and the corresponding bacterial viabilities (B) of *E. coli* and *S. aureus* in the presence of Cu-GMP/GODNF with different concentrations.

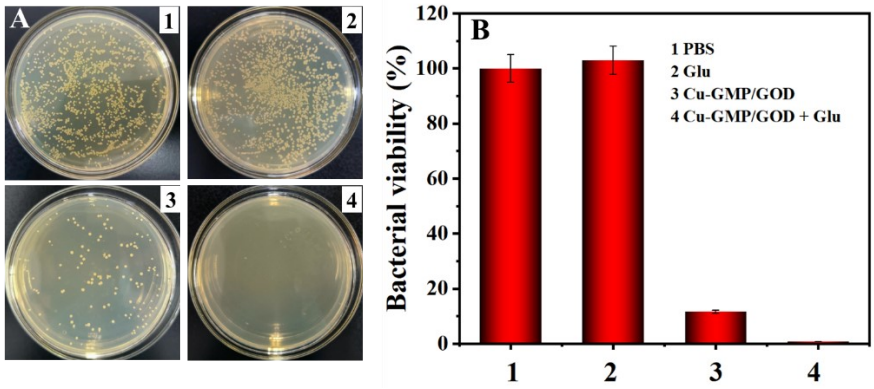


**Figure S14.** In vitro antibacterial efficacy of Cu-GMP/GODNF. Photographs of bacterial colonies formed (A) and the corresponding bacterial viabilities (B) of MRSA after different treatments.

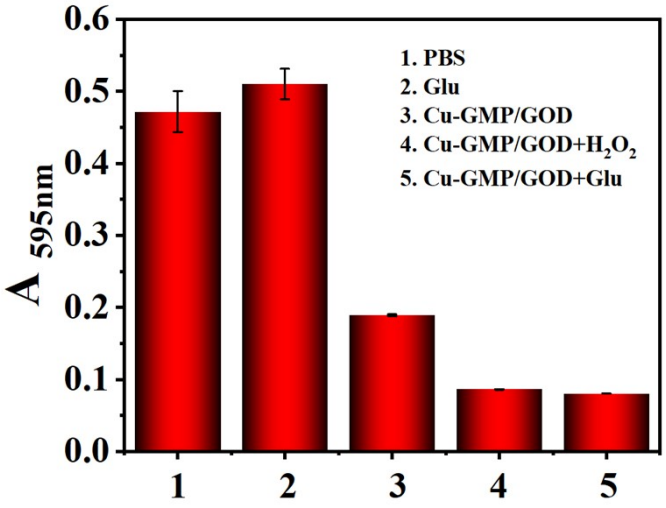


**Figure S15.** Biomass of MRSA biofilms under different treatments by measuring OD values at 595 nm.

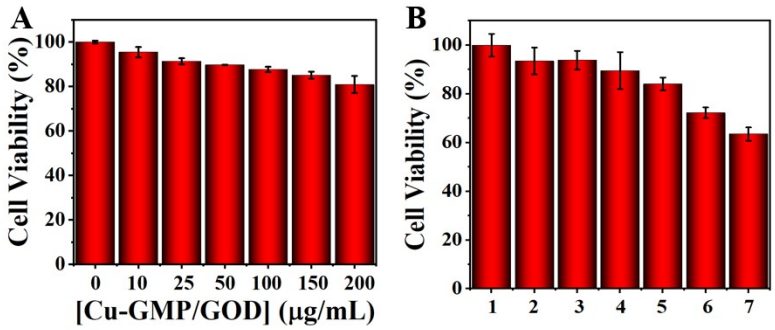


**Figure S16.** In vitro cell viability of L929 cells incubated with Cu-GMP/GODNF under different concentrations (A), and different treatments (1 PBS, 2 Cu-GMP, 3 Cu-GMP+Glu, 4 Cu-GMP/GODNF, 5 Cu-GMP/GODNF+1.0 mM Glu, 6 Cu-GMP/GODNF+2.0 mM Glu, 7 Cu-GMP/GODNF+5.0 mM Glu), the concentration of Cu-GMP and Cu-GMP/GODNF were 0.1 mg/mL, respectively (B).

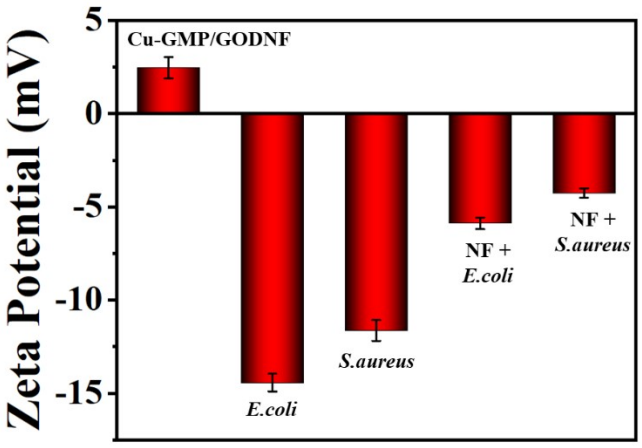


**Figure S17**. Zeta potential of bacteria before and after incubation with Cu-GMP/GODNF (1 mg $mL^{-1}$).

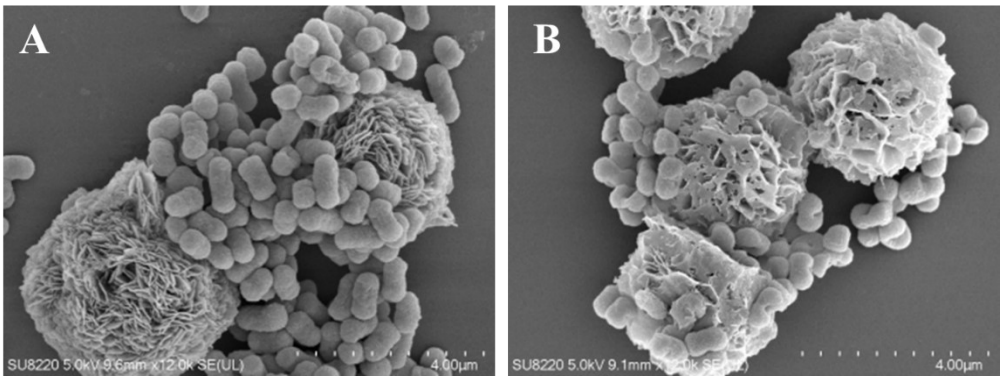


**Figure S18**. SEM images for verifying adhesion of Cu-GMP/GODNF to *E. coli* (A) and *S. aureus* (B).

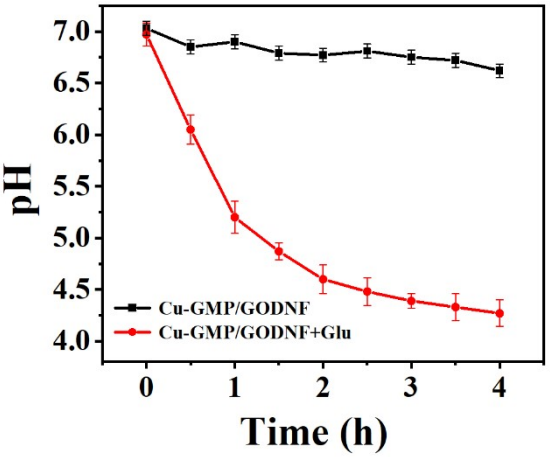


**Figure S19.** Changes in pH of bacteria after different treatments within 4 h.

**Table S1.** Kinetic parameters of Cu-GMPNF and NPs Cu-GMP/GODNF

| Nanozymes | TMB | | $H_2O_2$ | | Glu | |
|---|---|---|---|---|---|---|
| | $K_m$ (mM) | $V_{max}$ ($10^{-8}$ M/s) | $K_m$ (mM) | $V_{max}$ ($10^{-8}$ M/s) | $K_m$ (mM) | $V_{max}$ ($10^{-8}$ M/s) |
| Cu-GMPNF | 0.60 | 2.19 | 1.76 | 1.93 | | |
| Cu-GMP/GODNF | 0.23 | 0.783 | 2.83 | 4.59 | 1.78 | 1.04 |